Are Cambisols in Alpine Karst Autochthonous or Eolian in Origin

Author: Küfmann, Carola

Source: Arctic, Antarctic, and Alpine Research, 40(3) : 506-518

Published By: Institute of Arctic and Alpine Research (INSTAAR), University of Colorado

URL: https://doi.org/10.1657/1523-0430(06-091)[KUEFMANN]2.0.CO;2

Arctic, Antarctic, and Alpine Research, Vol. 40, No. 3, 2008, pp. 506–518

Are Cambisols in Alpine Karst Autochthonous or Eolian in Origin?

Carola Küfmann

Department of Geography, University of Munich (LMU), Luisenstrasse 37, 80333 Munich, Germany
carola.kuefmann@geographie.uni-muenchen.de

Abstract

This paper deals with a two-year study of karst soils and eolian dust deposition on the Reiteralpe paleosurface (1600 to 2000 m), Northern Calcareous Alps, Germany. Thirty soil profiles of Cambisols developed on Triassic and Cretaceous limestones are investigated. Dust samples collected periodically on snow cover provide influx rates and a seasonal dust record. Samples of soils, insoluble bedrock residue, and dust are characterized by pedological (e.g. grain size) and mineralogical (e.g. heavy minerals) data.

The data indicate that limestone subtypes with varying crack-fillings (ferrous clays) determine the colors and amounts of residue. Both correlate positively with the thickness of reddish Bo-horizons, supporting their autochthonous character. The topsoils, however, show substantial eolian addition (silt, fine sand, mica). In winter, far-traveled red Saharan dust without organic material prevails, carried to the area by strong foehn winds. In early springtime, browner dust (organic rich) is observed which contains periglacial silicate-rich detritus from regional sources such as the Crystalline Austrian Alps.

The measured winter dust influx rates are 4.8 cm per 10,000 years (related to 210 winter days). This is more than twice the calculated thickness of Holocene residue accumulation out of limestone weathering (2.3 cm per 10,000 years, related to 210 winter days), which indicates that eolian dust is a major contributor to alpine karst soil development.

DOI: 10.1657/1523-0430(06-091)[KUEFMANN]2.0.CO;2

Introduction

Available soil data are fragmentary in the high-mountain settings of the European Alps. With respect to altitude and geographic location, considerable differences exist concerning the quality and quantity of data. Detailed studies of soil types around timberline have been carried out in the crystalline Central Alps of Austria and Switzerland (e.g. Müller, 1986; Müller and Peyer, 1986; Mahaney et al., 1996; Veit and Höfner, 1993). Soil remnants on Tertiary paleosurfaces have also been studied recently in the Eastern Alps of Austria (e.g. Kuhlemann et al., 1999; Frisch et al., 2000). In contrast, there is little published information on mineral soil genesis in the alpine zone of the Northern Calcareous Alps (Mishra, 1982; Küfmann, 2003b). Although organic soils have been investigated in the subalpine zone, it was for understanding their influence on limestone solution (Hüttl, 1997; Credner et al., 1998).

The main reason for this paucity of data is the common view that mineral soil genesis on limestone is of minor importance in high alpine karst (e.g. Kubiena, 1953). This is due to climatically reduced dissolution rates and to the purity of limestones. Both control the amount of soil-forming residue (Coleman and Dethier, 1985; Drew, 1983). Therefore, distinct Bo horizons forming Chromic Cambisols are related either to colluvial processes (e.g. ''terra fusca'' according to Kubiena, 1953) or to Tertiary weathering products (e.g. ''terra rossa'' according to Kubiena, 1953).

An example of the latter is the interpretation of red clays as remnants of late Miocene soils (Kuhlemann et al., 1999). Due to their allochthonous character (e.g. loess-sized quartz silt; heavy minerals), some authors relate the origin of Cambisols to periglacial slope deposits of late glacial age (e.g. Haeberli, 1978; Mailänder and Veit, 2001). In contrast, an eolian origin of Cambisols has been proposed (e.g. Haeberli, 1978; Credner et al., 1998; Küfmann, 2003b). However, eolian deposition in alpine soils has been controversial (Littmann, 1991; Küfmann, 2003a), as the abundance of loess-sized silt is frequently ascribed to frost weathering and glacial grinding (French, 1976; Coutard and Francou, 1989; Matsuoka, 1990). However, a range of geomorphic mechanisms is capable of producing silt (Boulding and Boulding, 1981; Wright et al., 1998).

One important mechanism that has been overlooked is eolian activity producing desert loess of nonglacial origin (Wright, 2001a, 2001b). In the European Alps, desert loess is related to Saharan dust deposited as ''red dust'' or ''red snow'' (Mattson and Nihlén, 1996; Bücher and Dessens, 1999). In spite of the frequency of Saharan dust falls, only scattered data on influx rates exist (Wagenbach and Geis, 1989; De Angelis and Gaudichet, 1991; Schwikowski et al., 1995). These studies include estimates of aerosol deposition rates, but only for particular dust falls around a few stations at high elevations (>4000 m, e.g. French Alps). Nevertheless, they have provided the basis for a rough estimate of Saharan dust inputs. Precise rates of eolian input for longer periods based on measurements of influx rates do not exist. In particular, the Northern Calcareous Alps are a kind of ''terra incognita'' compared to work on eolian sediments in alpine soils of other regions (Thorn and Darmody, 1980, 1985; Litaor, 1987; Munn and Spackman, 1990; Dahms and Rawlins, 1996; Bockheim and Koerner, 1997; Muhs and Benedict, 2006).

The main reason for this gap is the widely accepted theory that eolian processes only play a minor role in soil genesis in high-mountainous karst (French, 1976). However, the discovery of

1523-0430/08 $7.00

loessic Cambisols in different parts of the Northern Calcareous Alps (Küfmann, 2003b) challenges this concept. Thus, the role of eolian inputs to alpine soils of this region needs to be reassessed.

A first contribution to the genesis of Cambisols on the Reiteralpe karst plateau is presented here. Soils, bedrock residues, and loessic deposits on snow cover are characterized by mineralogical and pedological data. Dust influx rates from two winter records (2002, 2003) are presented, quantifying the degree of eolian contribution to soil genesis in the study area.

Study Area

TOPOGRAPHY

The study area of Reiteralpe (Berchtesgadener Mountains, Northern Calcareous Alps) is located in the southeastern corner of Germany, close to the Austrian border. The central town is Berchtesgaden, 120 km southeast of Munich (48°08′N/11°35′E), the capital of Upper Bavaria (Fig. 1).

The study area in detail represents a Tertiary karst paleosurface (21 km^2) enclosed by high summits (1700 to 2300 m) and consists of the subalpine (1450 to 1900 m) and alpine (1900 to 2200 m) vegetation zones.

GEOLOGY

Triassic white Dachstein limestone ($CaCO_3 + MgCO_3 \geq 93\%$) is widespread, while remnants of Cretaceous (Lower and Middle Gosau) sediments cover only small areas due to erosion after tectonic uplift. Frost-weathered talus deposits and the debris of rock fans cover the surrounding steep slopes, and exposed beds of limestone comprise the syncline of the central karst plateau. A Pleistocene history of glaciation is documented by a polished glacio-karst relief and scattered local moraines.

FIGURE 1. Germany and the location of the study area (Maps of Germany, Munich 2007).

CLIMATE

On the karst plateau (station Traunsteiner Hütte, 1560 m), weather records are fragmentary but are continuously recorded at the nearby climatic stations at Predigtstuhl (1578 m) and Watzmannhaus (1820 m). The average annual air temperature at Predigtstuhl is 3.6°C and is 2.0°C at Watzmannhaus (data: German Weather Survey; period: 1979–1989). The climate is continental due to its interior location. Mean annual precipitation is 2215 mm on the central karst plateau (1560 m). Snow cover develops in October and is reduced between April and May. Nevertheless, 19 days with snow cover of more than 1 cm are commonly observed in May. The monthly distribution of wind frequency by direction indicates prevailing westerly and southerly winds (Table 1).

With respect to recent dust flux, the winds from westerly directions mainly transport humid air masses characterized by wet dust deposition. Prevailing southerly winds bring humid subtropical air, but dry air masses as well. Foehn winds over the Alps would favor dry deposition of dust. Southerly winds occur in every month. In particular, strong foehn winds (110–150 km h^{-1}) are often associated with heavy Saharan dust falls in spring and autumn (De Angelis and Gaudichet, 1991; Littmann, 1991; Küfmann, 2006).

VEGETATION COVER

Above treeline, the vegetation distribution shows associations of calcophile alpine meadows (*Caricetum firmae*, *Seslerio–Caricetum sempervirentis*, as well as *Caricetum ferrugineae*, *Laserpitio–Seslerietum*). In the subalpine zone, associations of shrubs and krummholz (*Erico–Rhododendretum hirsuti*, *Rhododendretum hirsuti–Mugetum sphagnetosum*, *Alnetum viridis*) prevail, along with subalpine forest with an uncommonly high proportion of *Pinus cembra* (*Vaccinio–Pinetum cembrae*, *Adenostyle glabre–Piceetum* caric. semp.). The patterns of vegetation and topoclimate create a mosaic of organic soil types (e.g. Humic Regosols, Rendzic Leptosols, and stages of Folic Histosols), while variations in geology and substratum strongly influence the distribution of autochthonous mineral soils.

Methods

FIELD METHODS

Soil data were collected from 30 profiles of mineral soils and their local bedrock along catenas from 1550 to 2000 m on the central karst plateau. Ten profiles were selected for presentation, reflecting the main distinct soil type groups (Tables 2 and 3).

The soil classification is based on the World Reference Base for Soil Resources (ISSS-ISRIC-FAO, 1998). The horizon nomenclature is that of FAO system (FAO/UNESCO/ISRIC, 1988–1997) and Soil Survey Staff (1994). Soil colors are characterized using the Munsell Soil Color Charts (KIC, 1990).

Eolian deposition was measured on snow cover at six main sample sites along the catena (C1). The dust samples were divided into four groups according to snow cover period:

Group 1: period of snow cover in the early winter season (October to November).
Group 2: period of snow cover in the high winter season (December to February).
Group 3: period of snow cover (October to February) with Saharan dust falls.

TABLE 1

Distribution of wind frequency by direction (%) at Watzmannhaus (1820 m) for 2002 (data: German Weather Survey, 2002).

	Jan.	Feb.	Mar.	Apr.	May	June	July	Aug.	Sept.	Oct.	Nov.	Dec.
N (315–45°)	1	15	19	41	22	24	28	32	26	4	3	4
E (45–135°)	19	12	5	9	15	11	16	15	15	17	26	29
S (135–225°)	48	34	43	33	35	21	14	26	17	41	35	35
W (225–315°)	32	39	33	18	28	44	42	28	42	38	36	33
Sum (%)	100	100	100	100	100	100	100	100	100	100	100	100

Group 4: period of reduced snow cover in the early spring season (April to June).

The dust samples were collected from the top of snow cover (0 to 1 cm thickness; 1 m^2 rectangles; methodology modified slightly from Thorn and Darmody, 1980). In each period of snow cover (group 1 to 4), all of the samples were collected in intervals of 10 to 15 days. They are assumed to represent the eolian dust concentrated on the snow surface by wind deposition. There is a lack of data in March due to high avalanche activity.

LABORATORY METHODS

Soil chemistry was determined using the following methods: pH (in 1N KCl, potentiometric method; Schlichting et al., 1995, p. 131), calcium carbonate (gasovolumetric method; Schlichting et al., 1995, p. 145), total organic carbon by wet oxidation (colorimetric $K_2Cr_2O_7$ method; Schlichting et al., 1995, p. 159), total nitrogen (Kjeldahl method; Schlichting et al., 1995, pp. 165–166), cationic exchange capacity (1N Na-acetate was used at pH 8.2).

The grain size (soils, bedrock residues, dust samples) was measured with a Sedigraph Laser Coulter LS 200 that comprises the grain sizes between 2000 and <2 μm (sand, silt, clay fractions). The samples were pretreated with HCl (10% solution) followed by a treatment with H_2O_2 (30% solution) to destroy organic material.

Alpine loess or eolian dust here is the total mineral dust fraction (μg; %) per sample, based on the non-soluble silicate content only. These organic- and carbonate-free sediments were isolated from each sample by the following procedures.

The snow samples were allowed to melt in plastic trashcans and the sediment gravity-settled. Bulk organic matter >2 mm (leaves, needles) was picked from the samples. Then, the sediment (mineral + organic matter <2 mm) in each sample was isolated by filtration (filter papers were oven-dried) and the oven-dried weights (at 60°C) were measured. After repeated treatment with H_2O_2 (10%) and washing, the oven-dried weights of inorganics (<2 mm) (μg; %) were determined. Finally, after treatment with HCl (10% solution), the weights of the total carbonates (μg; %) were also measured gravimetrically.

The following mineralogical data of soils and eolian sediments were determined (sample preparation methods: Allman and Lawrence, 1972; Moore and Reynolds, 1989):

(1) Quartz, feldspars, clay minerals by X-ray diffraction of the clay fraction including the qualitative and semiquantitative determination of the individual minerals (relative abundance based on X-ray diffraction peak height ratio).
(2) Major element analyses by wavelength-dispersive X-ray fluorescence.
(3) Heavy minerals.

The insoluble residues are the result of limestone solution and build up of the diagnostic Bo horizons of Chromic Cambisols (Kubiena, 1953). In the laboratory, the residues were gained by chemical separation of the non-carbonate minerals (e.g. clays, silicates) from the carbonate rocks. This was done by treating the crushed rock samples with HCl (10% solution) at room temperature for 24 hours (Ellingboe and Wilson, 1964). The insoluble residues were removed by filtering on previously dried and weighed filter paper. After washing and drying at 105°C, the residues were weighed. This separation was repeated until an adequate accumulation of residue had formed for further investigations (X-ray-diffraction, grain size measurement). Furthermore, microscopy (Leitz, 64 × 1.25; 80fold; Leitz Standard 18) and SEM-microscopy (SEM Leitz-AMR 1200) of dust particles were used. Mineralogy was determined in the total sand fractions, the coarse and medium silt classes (63 to 6.3 μm), and in the clay fraction (<2 μm). Due to varying mineral dust influx rates, the amounts of dust samples were sometimes too small. In these cases, particle size data and the mineralogical report (esp. heavy minerals) are not complete.

TABLE 2

Local description of selected soils on Reiteralpe.

Soil profile no.	UTM coordinates (m) (World Geodetic System 84)	Slope/aspect[1]	Altitude (m)	Karst morphology
P1	33 335404 E / N 5279133	2°/95°E	1702	karst hollow, glacio-karst
P2	33 333715 E / N 5277817	12°/135°SE	1970	inclined limestone pavement
P3	33 333535 E / N 5276278	5°/158°SSE	1622	lapies, glacio-karst
P4	33 333401 E / N 5276175	5°/180°S	1701	debris of rock fans
P5	33 334835 E / N 5278988	5°/135°SE	1620	exposed beds of limestone
P6	33 335167 E / N 5278922	5°/180°S	1720	dolines
P7	33 333577 E / N 5276224	10°/135°SE	1621	polished glacio-karst
P8	33 334809 E / N 5277328	5°/202°SSW	1570	inclined Gosau limestone
P9	33 334788 E / N 5277047	4°/23°NNE	1590	glacio-karst with sinkholes
P10	33 334875 E / N 5276631	2°/180°S	1557	glacio-karst with dolines

[1] Slope angle in degrees of soil profile/catena position and aspect of soil profile/catena position were measured using a clinometer (Necli) and a compass (Eschenbach).

TABLE 3

Main mineral soil types on Reiteralpe.

Profile	Horizon	Depth (cm)	R horizon[1]	Color[2] (wet)	Color[2] (dry)	Structure[3]	Texture[4]	Classification[5]
P 1/1	AB	0–2	dk, red marbled	10 YR 4/3	10 YR 6/3	1, f, gr	Silt	Eutric Cambisol
P 1/2	Bwo	2–14		7.5 YR 5/6	7.5 YR 6/4	2, sbk	SL	
P 1/3	R	>14						
P 2/1	ABwo	0–15	dk, red	7.5 YR 2/3	7.5 YR 3/3	2, f, sbk	SL	Eutric Cambisol, initial
P 2/2	R	>15						
P 3/1	Ah	0–2	dk, white	10 YR 2/2	10 YR 3/3	1, f, gr	Silt	Chromic Cambisol
P 3/2	Bo	2–20		7.5 YR 4/6	7.5 YR 6/6	2, f, sbk	SC	
P 3/3	R	>20						
P 4/1	Ah	0–2	dk, red, debris	10 YR 2/2	10 YR 3/3	1, f, gr	Silt	Chromic Cambisol *Terra fusca*[5]
P 4/2	Bo	2–30		5 YR 5/8	5 YR 6/8	2, f, abk	SCL	
P 4/3	BoC	30–50		2.5YR 4/6	2.5YR 6/4	2, m, sbk	SCL	
P 4/4	C	> 50						
P 5/1	Oa	0–3	dk, red marbled	10 YR 3/1	10 YR 3/2	sg, f	SL	Chromic Cambisol with folic O
P 5/2	Bwo	3–15		10 YR 3/6	10 YR 6/4	2, f, gr/sbk	SL	
P 5/3	R	>15						
P 6/1	AE	0–16	dk, wnc, brecc.	10 YR 3/4	10 YR 6/3	2, m, gr	L	Dystric Cambisol
P 6/2	Bwo	16–34		10 YR 5/8	10 YR 7/6	2, f, sbk	SCL	
P 6/3	R	>34						
P 7/1	Ah	0–5	dk, wnc	10YR 2/2	10YR 3/2	2, f, sbk	SL	Dystric Cambisol
P 7/2	Bwo	5–15		5YR 4/6	5YR 6/6	1, f, sbk	SCL	
P 7/3	R	>15						
P 8/1	AE	0–7	go, sandy, brecc.	10 YR 3/4	10 YR 6/3	1, f, gr	Silt	Ferralic Cambisol over initial Chromic
P 8/2	Bsh	7–10		10 YR 5/8	10 YR 7/6	2, f/m, sbk	L	Cambisol
P 8/3	2Bwo	10–25		10 YR 4/6	10 YR 6/6	2, f, sbk	SCL	
P 8/4	2Bo	25–30		7.5 YR 5/6	7.5 YR 6/6	2, f, abk	SCL	
P 8/5	R	>30						
P 9/1	Ah	0–16	go, marl	10 YR 4/3	10 YR 6/3	1, f, gr	Silt	Cambisol over Chromic Cambisol
P 9/2	Bw	16–35		10 YR 5/6	10 YR 7/4	1, f, gr	SL	
P 9/3	2Bo	35–55		10 YR 5/4	10 YR 7/4	2, f, abk	Clay	
P 9/4	R	>55						
P 10/1	Ah	0–8	go, lime, brecc.	10YR 2/2	10YR 3/2	1, f, gr	SL	Gleyi-Stagnic Cambisol
P 10/2	Bw	8–18		10YR 3/2	10YR 4/2	1, f, sbk	SCL	
P 10/3	Btx	18–45		10YR 4/4	10YR 6/4	2, g, abk	SC	
P 10/4	R	>45						

[1] dk = Dachstein limestone, solid (Triassic); brecc., brecciated; go = Gosau limestone, marly to sandy (Cretaceous); wnc, with nodular clay.
[2] Munsell Soil Color Charts (KIC, 1990).
[3] Grade: sg, single grain; 1, weak; 2, moderate; 3, strong. Size: f, fine; m, medium; c, coarse. Type: gr, granular; sbk, sub-angular blocky; abk, angular blocky.
[4] SL, Silt Loam; SC, Silty Clay; SCL, Silty Clay Loam; L, Loam.
[5] Classification and horizontation (FAO/UNESCO/ISRIC, 1988–1997; Soil Survey Staff, 1994; *Terra fusca* according to Kubiena, 1953).

CALCULATION METHODS

The calculations of mineral sedimentation rates are based on the silicate influx rates (μg cm^{-2} d^{-1}) per period and sample site. The calculated total winter sedimentation rate (μm per winter years [μm a^{-1}]) is divided into the period of snow cover development (160 days) and of snow reduction (50 days), according to climatic data. The calculations of recent sedimentation (μm) and of the potential postglacial eolian mineral sedimentation (cm per 10,000 years) are based on a bulk density

TABLE 4

Munsell colors of residue and corresponding soil horizon.

Parent rocks[1]	Color of insoluble residue of parent rock[1]		Color of corresponding residue horizons (Bo, Bwo)	
Dk, white	white	10 YR 8/1	very pale brown	10 YR 7/4
Dk, pinkish-white	pinkish white	7.5 YR 8/2	light yellowish brown	10 YR 6/4
Dk, red marbled	pink	5 YR 8/4	dark brown	7.5 YR 3/3
Dk, red to pinkish	reddish yellow	5 YR 6/6	reddish yellow	5 YR 6/8
Dk, red, brecciated	light red	2.5 YR 7/6	red	2.5 YR 4/6
Go, sandy brecciated	light reddish brown	5 YR 6/3	reddish yellow	5 YR 6/8
Go, marl	white	7.5 YR 8/1	reddish yellow	7.5 YR 6/6

[1] Mean: n = 10 samples per group; Go, Gosau limestone, marly to sandy (Cretaceous); Dk, Dachstein limestone (Triassic); colors according to KIC (1990).

TABLE 5

Mean grain size distribution of insoluble residue of limestone bedrock.

Rock sample[1]	Sand (2000–63 μm)	Silt (63–2 μm)	Clay <2 μm	Sum (%)	Silt to clay ratio	Texture[2]
Dk, white	0	65.0	35.0	100	1.8	loam
Dk, pinkish-white	0	67.8	32.2	100	2.1	loam
Dk, red marbled	0	66.3	33.7	100	2.0	loam
Dk, red to pinkish	31.9	48.3	19.8	100	2.4	silt loam
Dk, red, brecciated	41.3	44.4	14.3	100	3.1	sandy loam
Go, sandy, brecciated	17.9	62.2	19.9	100	3.1	silt loam
Go, marl	0	68.0	32.0	100	2.1	loam

[1] Mean: $n = 10$ samples per group; method: Laser Sedigraph; go, Gosau limestone, marly to sandy (Cretaceous); Dk, Dachstein limestone (Triassic).
[2] Texture category according to FAO/UNESCO/ISRIC (1988–1997).

of 1.3 g cm^{-3} for mineral silicate dust (Mattson and Nihlén, 1996) and an assumption that erosion by ice during the last glacial period removed preexisting soils. Furthermore, the following postglacial mean solution rates of limestone are used (bulk density: pure limestone of 2.65 g cm^{-3}; residue loam of 1.5 g cm^{-3}): 39 cm per 10,000 years for the upper subalpine zone (krummholz) and 34 cm per 10,000 years for the lower alpine zone. These solution rates are the result of a long-term field monitoring program (from 1995 to 2002) on karst plateaus in the Northern Calcareous Alps, which concentrated on the solution of limestones under soils (Hüttl, 1997, 1999; methodology: rock tablets from Trudgill, 1976).

Results

BEDROCK RESIDUE

In the field, the Triassic limestone shows significant micromorphological variations presumably due to tectonic movements. Several fault bundles cross the synclinal structure of Reiteralpe and lead to varying degrees of rock fracturing and highly jointed outcrops. These brecciated zones contain red clays and iron-rich sediment fillings. Thus, the white standard type of Dachstein limestone varies in color from pinkish to red. Associated Chromic Cambisols are characterized by similar reddish Bo horizons (7.5 YR 3/3; 5 YR 6/8; 2.5 YR 4/6). This similarity in color is also evident between most of the residue samples and corresponding Bo horizon (Table 4).

GRAIN SIZE DISTRIBUTION OF BEDROCK RESIDUE

The bedrock residues of white to red marbled Dachstein limestone are composed of fine silt with subordinate amounts of clay. In addition, sand (means: 31.9% to 41.3%) appears in the residues of brecciated types and in sandy Gosau limestone. The average content of coarse silt is 3%. The sand fraction contains fine and medium sand. The mean silt/clay ratio varies from 1.8 to 2.4 (Dachstein limestone) and is 3.1 in the residues of brecciated bedrock. The texture category is loam and either silty or sandy loam (Table 5).

MINERALOGY AND GEOCHEMISTRY OF BEDROCK RESIDUE

The major component of powdered rock samples (Dachstein limestone; Gosau series) is calcite with subordinate amounts of dolomite. Residues of purer limestone also reveal traces of hydrous mica and kaolinite (7 Å), while higher contents of kaolinite and illite appear in the reddish types. Some brecciated limestones also have siderite and ankerite. Chlorite is absent in all Triassic rock samples. Only three samples of Gosau indicate chlorite and sedimentary quartz (e.g. P 8/5; P 9/4). In many cases, the content of Fe_2O_3 refers to the intensity of reddish residue colors (Table 6).

The chemical data indicate average residue amounts of 10% to 11% in red to brecciated subtypes while the average of 2.1% appears in the residue samples of red marbled bedrock. This suggests a change in residue amounts with changes in underlying rock structures, which is also confirmed by the following correlation. The number of joints (% m^{-2}), measured on the outcrops adjacent to the soil profiles, shows positive correlation to the proportions of residue (%) in the underlying limestones (Fig. 2).

SOILS

On the central karst plateau, a variety of Cambisols (eutric, dystric, gleyi-stagnic) prevails. Their surface horizons are enriched

TABLE 6

Geochemistry of limestones and insoluble residues.

	Main components of limestones				Main oxides of the whole limestone		
Rock sample and Munsell color of its residue[1]	$CaCO_3$ (%)	$MgCO_3$ (%)	Residue (%)	Sum (%)	SiO_2 (%)	Al_2O_3 (%)	Fe_2O_3 (%)
Dk, white 10 YR 8/1	91.9	1.4	6.8	100	< 0.10	< 0.10	< 0.05
Dk, pinkish-white 7.5 YR 8/2	90.6	2.4	7.0	100	< 0.10	< 0.10	< 0.05
Dk, red marbled 5 YR 8/4	88.9	8.1	2.1	99.1	1.11	0.76	0.31
Dk, red to pinkish 5 YR 6/6	89.3	0.6	10.0	99.8	0.54	0.33	0.14
Dk, red, brecciated 2.5 YR 7/6	88.1	0.9	11.0	100	1.30	4.87	1.74
Go, sandy brecciated 5 YR 6/3	87.3	5.5	7.2	99.9	1.16	0.14	0.07
Go, marl 7.5 YR 8/1	84.3	6.5	9.2	100	0.18	0.16	0.09

[1] Mean: $n = 10$ samples per group; method: RFA and wet chemical analysis; go, Gosau limestone, marly to sandy (Cretaceous); Dk, Dachstein limestone (Triassic).

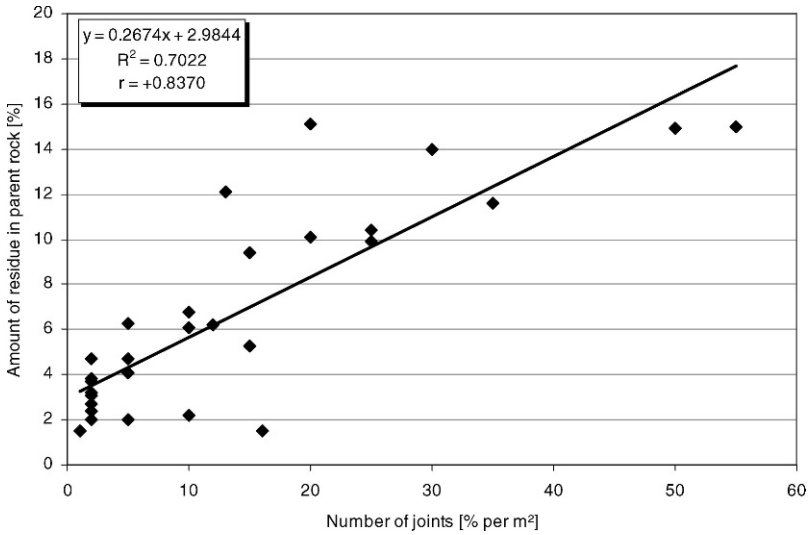

FIGURE 2. The relation between the number of joints (% m^{-2}) and the amounts of residue in the underlying rock ($n = 30$).

in silt and fine sand. Mica has accumulated in the A horizons, but it is also visible throughout the profiles. In relation to slope parameters and karst micromorphology, different genetic stages (initial, moderate, well-developed) of Cambisols exist for the field parameters of soil depth, horizontation, redness, and organic matter content. On dipped outcrops or inclined limestone pavement, initial Bo horizons are common, while in lapies and karst hollows, well-developed Chromic Cambisols occur. Gleyi-stagnic subtypes in sinkholes are related to a loamy substratum of Gosau marls or fragmentary till layers. Ferralic Cambisols are developed on Cretaceous Gosau marls and brecciated Gosau limestones with quartz-rich matrix.

GRAIN SIZE DISTRIBUTION OF SOILS

Grain size distribution (Fig. 3) shows textural differences between the topsoils and the subsurface horizons. High amounts of silt (mean: 66%; variation: 43% to 75%), notable fine sand (63 to 200 μm) and very fine sand (63 to 125 μm) with values between 13% and 44% prevail in the topsoil horizons (O, A, AE, and AB or B with eroded A). Fine sand and silt are also evident in the upper part of B horizons. Increasing proportions of medium and coarse sand appear in the B horizons of underlying sandy marls and brecciated limestone, whereas the B horizons developed on Dachstein limestone show a considerable range of clay content between 22% and 48%. Structural and textural differences between the Bw horizons (silt loam) and the 2Bo horizons (silty clay loam or clay) are obvious in pedon P8 with a sudden reduction in the sand fraction from 18% in Bsh to 8% in 2Bwo. A further example is pedon P9 with clay contents that increase from 22% in the Bw horizon to 35% in the 2Bo horizon.

The following mean values summarize the differences in grain size between topsoils and subsurface horizons:

Group G1: topsoil horizons (O, A, AE, AB):	sand 24%; silt 66%; clay 10%
Group G2: upper B horizons (Bw, Bsh, Bwo):	sand 16%; silt 63%; clay 22%
Group G3: subsurface Bo horizons (Bo, 2Bo):	sand 9%; silt 55%; clay 37%

Based on the grain size data, the mean ratios of coarse silt + fine sand/clay and silt/clay are given in Table 7.

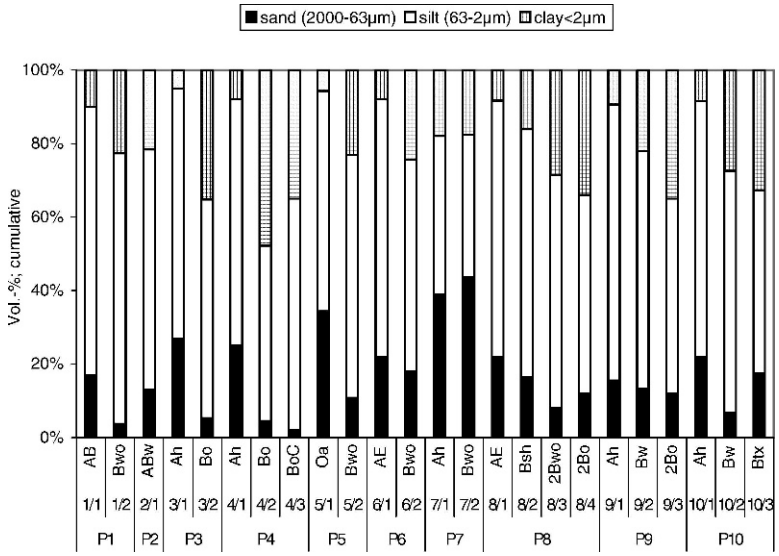

FIGURE 3. Grain size distribution of mineral soils.

TABLE 7

Grain size parameters of mineral soil (<2 mm) samples.

Characteristics	Horizon group	Main texture group[1]	Mean ratio silt / clay[2]	Mean ratio coarse silt + fine sand / clay[2]
G1: Topsoil horizons (mica and silt enriched)	O	S	8.2	8.8
	Ah	S	8.4	6.6
	AB	SL		
	AE	S	3.8	3.0
G2: Subsurface horizons (mixed with silt, sand)	Bw, Bhs, Btx	SL	3.0	1.4
	Bwo	SCL	2.3	1.0
G3: Subsurface horizons (loamy, clayey residues)	BoC	SCL, SC	1.8	0.4
	2Bo	C	1.0	0.2

[1] C, Clay; S, Silt; SL, Silt Loam; SC, Silty Clay; SCL, Silty Clay Loam.

[2] Calculation of means for each horizon group based on the particle size analysis of each single horizon sample of 30 soil profiles; e.g. silt content (%) / clay content (%).

The high silt/clay ratio of 8.4 in the topsoils decreases with soil depth. In contrast, the subsurface horizons of group 3 (G3 in Table 7), dominated by loamy to clayey residues from bedrock, have very low silt/clay and silt + fine sand/clay ratios.

SOIL CHEMISTRY

The soil A horizons have higher organic C contents than the subsurface horizons, as expected (Table 8).

However, humus coatings within the pores and patchy humus coatings along the profiles indicate translocation of organic matter into the B horizons. This is an indication of podzolization (e.g. in pedon P8). The mica-enriched A horizons (ochric, humic) and folic O horizons show acid reactions (pH 4.3 to 5.4). Accordingly, the soil carbonate content is low (variation: 0.9% to 4.4%). Higher values of $CaCO_3$ (variation: 3.1% and 10.3%) characterize the lower Bo horizons (pH: 6.1 to 7.0). Argillans in the Btx horizon (P10/3) indicate clay migration.

SOIL MINERALOGY

In general, distinct accumulations of minerals are found in the fine sand (125 to 63 μm) and in the silt fraction (63 to 6.3 μm) (Table 9).

The topsoil horizons (O, A, AE, AB) are dominated by biotite and muscovite (125 to 63 μm). The silt mineralogy shows dominant amounts of quartz and feldspars (orthoclase, albite). Subordinate minerals are micas, hornblende, calcite, and dolomite. The clay-size (<2 μm) minerals are dominated by illite and chlorite. Further characteristics include minor amounts of

TABLE 8

Selected chemical properties of Cambisols.

Profile	Horizon	Depth (cm)	pH (1n KCl)	$CaCO_3$ (%)	OC (%)	Total N	C:N	CEC (cmol [+] / kg)
P 1/1	AB	0–2	5.1	0.9	1.9	0.15	13	4.6
P 1/2	Bwo	2–14	5.3	0.7	1.1	0.23	5	6.7
P 2/1	ABW	0–15	6.7	4.4	15.0	1.27	12	12.9
P 3/1	Ah	0–2	5.1	1.2	3.0	0.26	11	9.6
P 3/2	Bo	2–20	7.0	10.3	2.2	0.29	8	8.5
P 4/1	Ah	0–2	5.1	1.8	4.5	0.46	10	5.9
P 4/2	Bo	2–30	5.3	3.1	3.0	0.20	15	5.6
P 4/3	BoC	30–50	6.4	3.8	2.0	0.11	18	3.2
P 5/1	Oa	0–3	5.0	2.9	17.5	1.35	13	16.7
P 5/2	Bow	3–15	6.4	3.4	3.6	0.46	8	10.1
P 6/1	AE	0–16	4.5	1.0	5.9	0.51	12	5.9
P 6/2	Bwo	16–34	6.4	3.3	1.8	0.15	12	5.3
P 7/1	Ah	0–5	5.4	4.2	5.6	0.32	17	15.2
P 7/2	Bwo	5–15	6.8	7.9	3.0	0.20	15	12.6
P 8/1	AE	0–7	4.5	1.0	13.5	0.90	15	7.3
P 8/2	Bsh	7–10	4.3	1.6	3.9	0.32	12	6.2
P 8/3	2Bwo	10–25	4.4	1.7	1.8	0.14	13	4.8
P 8/4	2Bo	25–30	6.5	3.1	1.5	0.15	10	14.6
P 9/1	Ah	0–16	4.3	2.0	7.6	0.84	9	7.6
P 9/2	Bw	16–35	4.1	0.9	2.9	0.25	12	5.0
P 9/3	2Bo	35–55	6.1	8.9	1.6	0.08	20	8.6
P 10/1	Ah	0–8	4.6	3.1	3.3	0.29	11	9.6
P 10/2	Bw	8–18	4.6	4.5	1.4	0.20	7	7.2
P 10/3	Btx	18–45	5.8	6.5	1.2	0.11	11	7.3

TABLE 9

Relative abundance of minerals in soil horizons.

	Grain size fractionation of minerals			
Mean relative abundance[1] in:	Fine sand (125–63 μm)	Coarse silt (63–20 μm)	Medium silt (20–6.3 μm)	Clay (<2 μm)
Topsoil horizons (O, A, AE, AB)				
Dominant (+++)	micas[2]	quartz, fsp[3]	quartz	illite
Major (++)	quartz, hm[4]	micas, hbl[4]	fsp, cc, dol[5]	chlorite
Minor (+)		cc, fsp	fsp, chlorite, dol	kaolinite, ML_{illite}[6]
Traces				cc, dol, gypsum, hematite, smectite
Subsurface horizons (Bw, Bhs, Btx, Bwo, Bo)				
Dominant (+++)				illite
Major (++)		micas, hbl	quartz, fsp	ML_{illite}, chlorite
Minor (+)	quartz, hm	hm	chlorite	kaolinite
Traces				smectite, dol
Subsurface horizons (2Bo, BoC)				
Dominant (+++)				kaolinite
Major (++)		cc		illite, chlorite
Minor (+)	cc			
Traces	hm	quartz, fsp	quartz, fsp	gibbsite

[1] Methods: X-ray diffraction (relative abundances based on X-ray diffraction peak height), mean: XRF-pattern of 5 single samples per horizon group; microscopy of the sand fraction.

[2] micas: biotite, muscovite, biotite > muscovite.

[3] fsp, feldspars: albite and orthoclase, albite > orthoclase.

[4] hm: heavy minerals; hbl, hornblende green and brown.

[5] cc, calcite; dol, dolomite.

[6] ML_{illite}: mixed-layer clay minerals, interstratified illite-smectite with illite (>60 rel.-%).

kaolinite, mixed-layer material, as well as traces of dolomite and calcite. Two samples of A horizons (P1/1; P7/1) also show traces of gypsum, hematite, and smectite.

The sand mineralogy of the subsurface B horizons (Bw, Bhs, Btx, Bwo) reveals heavy minerals and quartz. In the silt fractions quartz, feldspars, micas, and heavy minerals are abundant, but decrease significantly with soil depth reaching a minimum in the Bo horizons. The major clay mineral in the upper B horizons is illite with lesser amounts of mixed-layer material and chlorite. Illite or kaolinite are dominant in the lower Bo horizons.

In contrast, the 2Bo horizons only show grains of heavy minerals (125 to 63 μm), quartz, and feldspars (63 to 6.3 μm). Varying amounts of calcite are the result of incorporated bedrock material (e.g. P8/4, 2Bo). The major clay mineral here is kaolinite with subordinate illite. Finally, the X-ray diffraction patterns of pedon 9 demonstrate the differences in clay mineralogy with soil depth (Table 10). The distribution of heavy minerals shows high amounts of hornblende, epidote, and zoisite, totaling more than 50% (Table 11).

A higher number of rounded zircon grains with scarred surfaces and quartz prevail in the folic O horizons and acid B horizons. The upper parts (5 to 10 cm) of humic A horizons and folic O horizons also show different amounts of garnet varying with soil pH. This can also be observed in Ferralic Cambisols (AE horizons: mean pH: 4.6; B horizons: mean pH: 4.9) and in Dystric Cambisols (A horizons: mean pH: 5.0). The diminution of garnet goes hand in hand with a significant increase of weathered hornblende. Topsoils and B horizons display similar spectra with regard to heavy mineral contributions. On the other hand, the Bo horizons show insignificant quantities of heavy minerals with statistically invalid grain populations (<50 grains).

Moreover, the data of X-ray fluorescence analysis indicate a dominance of SiO_2 (mean: 60%; variation: 45% to 62%) in the topsoils and in most of the upper B horizons. In contrast, high values of CaO + MgO (%) characterize the 2Bo horizons, which have often more than twice the value of the carbonate content of the upper Bw horizons.

SOIL DEPTH AND AMOUNTS OF RESIDUE

Field observations indicate that the thickness of Bo horizons (1 to 5 cm) is significantly lower on solid pure white Dachstein limestone and is greater in soils developed on brecciated rocks. The presumed influence of rock purity is indicated by the following relation between the depth of overlying Bo horizons (cm) and the proportion (%) of insoluble residue of each R horizon, yielding in a strong positive correlation (Fig. 4).

This correlation is strongest when the influence of colluvial mixing is excluded (e.g. fillings in faults, karst hollows). Therefore,

TABLE 10

Percentages of layer silicates (clay fraction < 2 μm) estimated from areas under X-ray diffraction peaks (summed to 100%).

Sample	Clay minerals [rel.-%]; clay fraction <2 μm			
Pedon P 9 Cambisol over Chromic Cambisol	ML_{illite}[1]	Illite	Kaolinite	Chlorite
P 9/1 Ah (0–16 cm)	10	40	8	42
P 9/2 Bw (16–35 cm)	22	30	15	33
P 9/3 2Bo (35–55 cm)	8	28	40	24
P 9/4 R (> 55 cm) residues of Gosau marl	0	63	10	27

[1] ML_{illite}: mixed-layer clay minerals, interstratified illite-smectite with illite (>60 rel.-%).

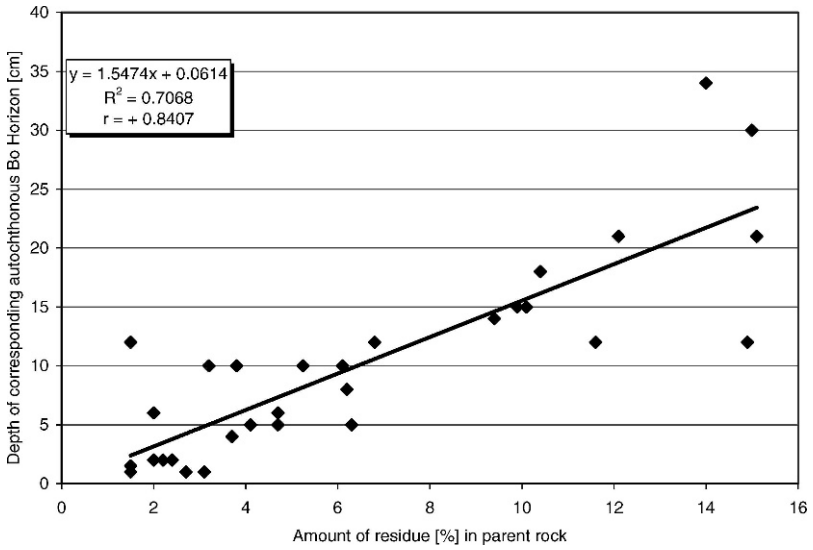

FIGURE 4. The relation between the depth of Bo horizons (cm) and the amounts of residue in the underlying rock ($n = 30$).

the field data only include profiles on solid limestone. The lithogenetic control of the Bo horizons is further underscored by a comparison of the measured soil depth data with the potential calculated thickness (cm) of residue layers built up over a time span of 10,000 years. The estimate of 10,000 years is based on the glacial history of the study area, since the entire region was glaciated during the last glacial period (Wisconsin/Weischelian), and deglaciation occurred about 10,000 years ago (Fischer, 1988).

The calculated thickness of a residue layer built up over a time span of 10,000 years would be in the range of 1.3 to 4.1 cm, depending on the purity of solid Dachstein limestone types. This calculation is based on a postglacial limestone solution rate of 34 cm per 10,000 years (see *CALCULATION METHODS* in this paper). However, the average measured soil depth on the red and brecciated outcrops (10 to 25 cm) is significantly higher than the calculated ones (Table 12).

EOLIAN DUST ON SNOW COVER

The seasonal record of eolian deposition on snow cover indicates that the winter dust samples (Group 1 and 2: October to February) are of brown to reddish color (7.5 YR 4/3; 10YR 3/2; 10YR 5/2; 10YR 6/3). Remarkable red dust (5 YR 4/2; 5YR 4/4; 5YR 5/6) is recorded following periods with strong southerly winds (Group 3). In contrast, dust of samples taken in the early spring period (Group 4a: April to June) is generally browner and obviously contains organic material. Nevertheless, reddish dust deposits also appear during the spring melt period (Group 4b: April to June), again observed following periods with southerly foehn winds.

GRAIN SIZE DISTRIBUTION OF EOLIAN DUST

The mean grain size data (Table 13) indicate that the dust deposits are composed predominantly of silt (65% to 85%) with varying proportions of clay and fine sand. Medium sand (630 to 200 μm) only appears in the spring samples. In contrast, the grain size of red dust deposited during winter is finer, showing higher amounts of particles between 20 and 2 μm (>57% fine silt of the total silt fraction) and average clay contents of 16%. Striking high values of coarse silt (mean: 45%) appear in the reddish springtime samples, suggesting a mixture of two different dust sources.

The measured mean dust influx rates are 12 $mg \cdot m^{-2}\ d^{-1}$ (variation: 0.7 to 55 $mg \cdot m^{-2}\ d^{-1}$) during snow cover development

TABLE 11

Mean distribution of heavy minerals in selected soil horizons.

Mean total spectrum of heavy minerals (amount of grains %); fraction 0.1–0.25 mm (n = 5 of each soil horizon group)											
Samples	G	Z	T	R	Ap	St	Di	Hbl	Ep+Zo	Chl	Grain sum
G1: Topsoil horizons (mica and silt enriched)											
O of Cambisols, Regosols (folic)	14	22	6	4	3	3	0	18	30	0	130*
Ah of Cambisols (eutric, chromic)	35	7	0	2	0	2	0	25	29	0	300
Ah of Cambisols (dystric)	8	4	1	1	0	1	0	38	46	1	300
AE of Ferralic Cambisols	2	3	1	1	1	1	0	36	55	0	300
G2: Subsurface horizons (mixed with silt, sand)											
AB, Bw	37	11	5	8	1	2	2	5	29	0	200
Bsh	2	2	1	0	2	2	1	54	29	7	200
G3: Subsurface horizons (loamy, clayey residues)											
Bo and Bow	grains: 14 garnet, 3 zircon, 1 rutile, 1 staurolite, 5 Hbl										
2Bo	grains: 2 zircon, 4 rutile, 1 staurolite										

G = garnet; Z = zircon (+ xenotime + monazite), T = tourmaline, R = rutile, Ap = apatite, St = staurolite, Di = disthene, Hbl = hornblende, Ep+Zo = epidote + zoisite (+ clinozoisite + sometimes fine-grained aggregates of pumpellyite), Chl = chlorite and chloritoides;

* Lower grain sum due to small quantities of material or to protracting extraction of organic matter in O horizons.

TABLE 12

Postglacial (~10,000 years) soil depth of Bo horizons.

Parent underlying rocks (R horizon)	Measured soil depth of Bo horizons (cm)[1]			Calculated potential soil depth (cm)[2]
	Min.	Max.	Mean	
Dk, white to pinkish	1	10	5	4.1
Dk, red marbled	3	20	15	1.3
Dk, red to pinkish	4	22	16	6.0
Dk, red, brecciated	10	30	25	6.7
Go, sandy	3	15	10	4.3

[1] Bulk density: residue loam: 1.5 g cm^{-3}; limestone: 2.65 g cm^{-3}.

[2] Based on the mean postglacial limestone solution rate of 34 cm per 10,000 years (lower alpine zone; from Hüttl, 1997, 1999).

and 64 $mg \cdot m^{-2}\ d^{-1}$ (variation: 8 to 135 $mg \cdot m^{-2}\ d^{-1}$) during springtime. Accordingly, the calculated sedimentation rates yield 0.6 μm during the sample period "winter" (160d) and 4.2 μm during the sample period "springtime" (50d).

MINERALOGY AND GEOCHEMISTRY OF EOLIAN DUST

The wet chemical analysis of winter samples (December to February) reveals solely mineral dust (mean value of silicates: 96%; variation: 93% to 99%) with a total content of carbonates of only 4% (variation: 1% to 7%). In contrast, the samples of October and May obviously contain organic material (mean: 21%; variation: 10% to 32%) with humus colloids (<2 mm), bacteria, spores, pollen, and fungal hypha.

During the period of melting, organic matter increases further (mean: 37%; variation: 32% to 43%), leading to darker colors (7.5 YR 3/1; 10YR 2/1; 10YR 2/1; 10YR 3/1). Characteristics here are: organic detritus (>2 mm), pollen of alpine (e.g. *Caricetum firmae*, *Aster alpinus*) and subalpine forest flora (e.g. *Abies alba, Pinus mugo*), and fragments of alpine insects (e.g. *Svaeva pyrastri*, *Volcucella pellucens* etc.).

Quartz with subordinate amounts of feldspar and mica is the most abundant mineral component in all samples (Table 14). Both calcite and dolomite are identified in most X-ray diffraction patterns but in minor quantities. Additionally, traces of hematite, gibbsite, kaolinite, and heavy minerals are obvious in the red dust samples, as well as fragments of diatoms and rounded quartz grains with iron hydroxide coatings (quartz group I). A striking change is observed in the mineral composition of early springtime samples with a prevalence of angular fragments of quartz (quartz group II), brown and green hornblende, micas, and heavy minerals (e.g. disthene, garnet).

Discussion

The Cambisols on Reiteralpe are interpreted to be predominantly autochthonous, at least for their subsoils. The variety of brown to reddish B horizons corresponds to the residue substratum of limestone subtypes showing different degrees of fracturing and joint-fillings with reddish, ferrous clays. Therefore, the rubification of the Bo horizons is mostly inherited from the subjacent bedrock, generated during pedogenic decalcification of limestone.

Both the lower Bo horizons and their bedrock residues show illite and kaolinite as major autochthonous components of the clay fraction. However, chlorite is often found in the upper B horizons, but is absent in all samples of Triassic limestone. In karst hollows, some soil fillings (e.g. P1) show high amounts of Fe_2O_3, Al_2O_3, and kaolinite which may also reflect Tertiary subtropical weathering as alluded to in other soil studies (Frisch et al., 2000).

In general, the grain size distributions of the residue samples correspond closely with the Bo horizons concerning the clay contents. However, several soil samples also indicate clay migration. According to some workers (e.g. Bockheim and Koerner, 1997), this process sometimes occurs beneath krummholz. Therefore, clay migration may be associated with *Rhododendretum hirsuti–Mugetum sphagnetosum* in the study area.

The measured soil depth of Bo horizons is mostly in accordance with the amounts of residue content of parent bedrock, provided the soil site was without colluvial contaminants. This further suggests that the lower B horizons are formed by limestone solution. Variations in soil depth may be related to microtopography (e.g. in karst hollows, dolines), slope movement processes by solifluction, and soil creep as well as varying limestone solution rates during the Holocene.

Nevertheless, soil thickness appears to be controlled to a greater degree by eolian deposition. A gradient of loessic influence

TABLE 13

Mean grain size distribution of seasonal dust samples on snow cover (without interval 2000 to 630 μm, as coarse sand is not existing).

Dust samples	Grain size (vol.%) measured by Laser Sedigraph[1]							
	m sand 630–200 μm	f sand 200–63 μm	c silt 63–20 μm	m silt 20–6.3 μm	f silt 6.3–2 μm	clay >2 μm	Sum silt 63–2 μm	Texture[2]
G1: Early winter (Oct. to Nov.)	0.0	5.9	32.0	31.7	20.6	9.8	84.3	silt loam
G2: High winter (Dec. to Feb.)	0.0	6.6	31.9	28.2	21.4	12.0	81.5	silt loam
G3: Red far-traveled dust (Dec. to Feb.)	0.0	6.6	19.9	27.4	29.9	16.2	77.2	silt loam
G4a: Melting period (Apr. to June)	9.5	14.9	23.1	24.8	17.4	10.3	65.3	sandy loam
G4b: Reddish dust (Apr. to June)	0.0	9.2	45.2	27.6	12.6	5.4	85.4	silt

[1] n = 5 single samples per sample category; c = coarse; m = medium; f = fine.

[2] Texture category according to FAO/UNESCO/ISRIC (1988–1997).

TABLE 14

Mineral properties of eolian dust samples.

Sample group (October to February; $n = 14$)	Main grain size interval (μm)
—Calcite, dolomite	<10; <20
—Mica (biotite, muscovite); all stages of mica decay	63–20; <20
—Dominance of quartz group I: rounded quartz (yellow, gray) with iron hydroxide coatings	63–20; <20
—Angular fragments of quartz partly with coatings	≤20
—Feldspars (orthoclase, albite), fresh to hardly weathered	≤20
—Chlorite, gibbsite, kaolinite, illite, traces of hematite	<10
—Heavy minerals (dominance of zircon, rutile, tourmaline, green hornblende)	100–250
Fragments of diatoms	<2000
Sample group (April to June; $n = 14$)	Main grain size interval (μm)
—Calcite, orthoclase, mica (angular fragments of biotite), non-weathered hornblende (green and brown)	20–6,3; 125–63; 63–20
—Dominance of quartz group II: angular fragments of quartz (white)	125–63; 63–20
—Illite, kaolinite	<20
—Heavy minerals (dominance of garnet, staurolite, disthene, epidote-zoisite-group)	100–250
Fragments of diatoms	<2000
Methods: X-ray diffraction, microscopy, heavy minerals	

can be observed when comparing mineralogical und pedological data from eolian dust samples, soils, and limestone residues. Silt, fine sand, mica, and heavy minerals are enriched in topsoil horizons (O, Ah, and AE horizons), indicating a strong recent eolian influence. The silt produced from local limestone by frost action is negligible. Quartz, feldspars, mica, chlorite, and heavy minerals are also common in the upper B horizons, which suggests eolian mixing. However, chlorite in ferralic B horizons may also reflect the transformation of illite (poor in potassium) into soil chlorite as a result of acidic soil conditions.

Finally, textural changes (e.g. from silt to silty clay; from silt loam to clay) in B horizons and a striking diminution of heavy minerals indicate a strong residue influence in lower horizons (Bo, 2Bo). The sequence ''loessic deposits over autochthonous residues'' is represented by an abrupt boundary from the upper B horizons to the 2Bo horizons overlying the limestone.

According to other studies (Reheis and Kihl, 1995; Bockheim and Koerner, 1997), sand accumulation in surface horizons can be a local eolian signature. On Reiteralpe, the prevailing fine and very fine sand (125 to 63 μm) additions to the topsoils are interpreted to be of regional eolian origin, as the red Saharan dust is not likely to have any sand in it. Quartz, feldspars, mica, and heavy minerals (garnet, hornblende, epidote, zoisite) indicate silicate-rich detritus from the Crystalline Austrian Alps. On the other hand, the abundance of coarse and medium sand in Ferralic Cambisols indicates *in situ* weathering of brecciated and sandy Gosau limestone.

The data presented here indicate that the distribution of heavy minerals, quartz, and feldspars, as well as the geochemistry (e.g. SiO_2; Al_2O_3), are distinct parameters in karst soils for estimating both the loessic and residue contribution along the soil profiles (Thorn and Darmody, 1985; Dahms, 1993). Additionally, the silt/clay ratio was used for completing the genetic interpretation. The mean values of the ratio only show marked differences between the topsoils (e.g. 8.4) and the 2Bo horizons (e.g. 1.0). However, the decreasing values within the eolian mixed upper B horizons are not rigorous enough for determining different stages of eolian influence as both local eolian (higher silt content and fine sand) and far-traveled dust (fine grained, higher clay percentages) are incorporated.

Dust samples collected periodically in the study area provide a seasonal record of dust deposition. Their variations of chemical components can be related to dust sources and transport patterns, as discussed by Avila et al. (2007).

On Reiteralpe, the distribution of heavy minerals and the chemical compositions (proportion of silicates) of both soils and eolian dust reveal two main dust sources interacting seasonally with weather conditions and regional snow cover development. Most of the present-day loess is derived from regional (50 to 500 km) crystalline dust sources south of the study area (e.g. Central Alps, Austria; Southern Alps, Italy). At high elevations (up to 3700 m), glacial outwash and periglacial frost weathering produce silt and fine sand. In winter, when local source areas are snow covered, southerly winds transport Saharan dust to the region. Mineralogy and grain size distribution of most of these red dust samples is similar to those recorded in other published data on Saharan dust analysis (e.g. Bücher and Dessens, 1999; Pye, 1992).

As discussed by Wagenbach and Geis (1989), southerly winds accumulate dust on snow mainly by dry deposition. On Reiteralpe, melting water is the main secondary dust transport mechanism into soils. Here, alpine meadow vegetation plays a major role in trapping the loessic deposits that favor the development of acidophile plant associations with *Carex ferruginea*, *Huperzia selago*, and *Rhododendron ferrugineum*.

The sedimentation rates measured at Reiteralpe are in good agreement with other eolian measurements taken in alpine or

TABLE 15

Eolian sedimentation rates from subalpine and alpine areas (varying methods and sample material).

Study area	Sedimentation rate (μm a^{-1} or cm·10 Ka^{-1}]	Sample method	Literature
Reiteralpe, Northern Calcareous Alps:			
A) Snow cover period ''winter'' (160 days)	0.1–0.8 (mean: 0.6)	dust on snow covers	Küfmann (this paper)
B) Melting period ''springtime'' (50 days)	3.0–5.3 (mean: 4.2)	dust on snow covers	Küfmann (this paper)
C) Dust flux ''summer''	3.1–9.8 (mean: 4.2)	dust from rain (using dust boxes)	Küfmann (2003a)
Wind River Range, U.S.A., alpine zone	0.1–7.4	dust from rain and on snow covers	Dahms and Rawlins (1996)
Swiss Alps, nival zone (>3800 m)	0.5	Saharan dust, deposits on glaciers	Wagenbach and Geis (1989)

subalpine settings, although methodology often varies (Table 15). Based on the measured influx rates, the sedimentation rate per winter season is 4.8 μm (210 days). This is more than twice the calculated thickness of residue accumulation out of limestone solution (2.3 μm, related to 210 winter days). Taking the summer dust rate of 4.2 μm into account, measured using dust boxes (Küfmann, 2003a), the eolian contributions result in an annual loess layer of 9.0 μm. Based on the somewhat simple assumption that no material is lost either by erosion or by leaching, this loess accumulation rate yields a layer about 9.0 cm thick in 10,000 years. Compared to the calculated means of Holocene residue accumulation out of pure white to pinkish Dachstein limestone (4.1 cm per 10,000 years), eolian deposition is a significant process in alpine karst soil genesis.

Conclusions

The initial question of whether Cambisols in alpine karst are autochthonous or eolian in origin cannot be answered with a simple ''yes'' or ''no.'' The Cambisols developed on solid Triassic and Cretaceous limestones are of autochthonous origin with respect to their lower Bo horizons. Their color, thickness, mineralogy, and grain size correspond to the residues of local bedrock. The residual origin of the reddish soils depends on the tectonic development of Reiteralpe karst plateau, as different subtypes of the standard type of white Dachstein limestone were examined. Varying degrees of fracturing and crack-fillings with red iron-rich clays characterize brecciated, red marbled, and red limestone subtypes.

A major eolian contribution is identified in the topsoils from the presence of silt, fine sand, mica, quartz, and heavy minerals. This allochthonous material is also incorporated in the upper B horizons but decreases with soil depth. Therefore, the solum of the upper Bwo horizons often is a mixture of loessic deposits with autochthonous bedrock residue.

The seasonal dust record of eolian dust on snow cover indicates dust from different areas. In winter, red Saharan dust prevails, carried to the study area by strong southerly foehn winds. These midwinter dust inputs are dominated by mineral particles. The springtime dust samples (April to June) are browner and contain much more organic material, such as pollen and plant detritus. With regard to the mineral components, a striking change appears in the transition from winter to spring. Angular fragments of quartz, green hornblende, micas, and heavy minerals reveal loessic dust derived from alpine sources with silicate-rich rock formations (distance: >50 to 200 km; Austrian Crystalline Alps).

The measured winter dust influx rates are 4.8 cm per 10,000 years (related to 210 winter days). This is more than twice the calculated thickness of Holocene residue accumulation out of limestone dissolution (2.3 cm per 10,000 years, related to 210 winter days), indicating that eolian dust is a major contributor to alpine karst soil development.

Summing up, the investigation of soil, bedrock residues, and eolian deposits in combination with a seasonal dust record illustrates the fundamentals of present-day eolian dynamics (dust origin, transport, sedimentation) in the alpine karst of the Northern Calcareous Alps.

Acknowledgments

The Deutsche Forschungsgemeinschaft (DFG, Bonn, Germany) provided financial support. Thanks are given to Dr. M. Vogel (National Park Berchtesgaden) for data support and OStR F. Kneissl for logistic knowledge. Great thanks go to the students S. Burig, L. Duffy, K. Kothieringer, A. Rappl, and T. Rauch for laboratory and field support. Prof. Dr. H. Schmid and Dr. U. Rast (Geological Survey, Munich) provided analytic support. Many thanks are given to Dipl.-Ing. A. Küfmann for layout support and reviewing the English manuscript.

References Cited

Allman, H., and Lawrence, P., 1972: *Geological laboratory techniques*. London: P. Blandford.

Avila, A., Alcarón, M., Castillo, S., Escudero, M., García Orellana, J., Masqué, P., and Querol, X., 2007: Variation of soluble and insoluble calcium in red rains related to dust sources and transport patterns from North Africa to northeastern Spain. *Journal of Geophysical Research*, 112: D05210, doi: 10.1029/2006JD007153.

Bockheim, J. G., and Koerner, D., 1997: Pedogenesis in alpine ecosystems of the eastern Uinta Mountains, Utah, U.S.A. *Arctic and Alpine Research*, 29(2): 164–172.

Boulding, B. H., and Boulding, J. R., 1981: Genesis of silty and clayey material in some alpine soils in Teton Mountains, Wyoming and Idaho. *Indiana Academy of Science Proceedings*, 91: 552–562.

Bücher, A., and Dessens, J., 1999: Poussières Sahariennes sur la France et l'Angleterre, 6–9 Mars 1991. *The Journal of Meteorology*, 17: 226–233.

Coleman, S. M., and Dethier, D. P., 1985: *Rates of chemical weathering of rocks and minerals*. Orlando: Academic Press Inc.

Coutard, J.-P., and Francou, B., 1989: Rock temperature measurements in two alpine environments: implications for frost weathering. *Arctic and Alpine Research*, 21(4): 399–416.

Credner, B., Hüttl, C., and Rögner, K., 1998: The formation and distribution of soils and vegetation at the Zugspitzplatt (Bavaria, Germany) related to climate, aspect, and geomorphology. *Ecologie*, 29(1–2): 63–65.

Dahms, D. E., 1993: Mineralogical evidence for eolian contributions to soils of late Quaternary moraines, Wind River Mts., Wyoming, USA. *Geoderma*, 59: 175–196.

Dahms, D. E., and Rawlins, C. L., 1996: A two-year record of eolian sedimentation in the Wind River Range, Wyoming, USA. *Arctic and Alpine Research*, 28: 210–216.

De Angelis, M., and Gaudichet, A., 1991: Saharan dust deposition over Mont Blanc (French Alps) during the last 30 years. *Tellus*, 43B: 61–75.

Drew, D. P., 1983: Accelerated soil erosion in a karst area: The Burren, western Ireland. *Journal of Hydrology*, 61: 113–124.

Ellingboe, J., and Wilson, J., 1964: A quantitative separation of non-carbonate minerals from carbonate minerals. *Journal of Sedimentary Petrology*, 34(2): 412–418.

FAO/UNESCO/ISRIC, 1988–1997: Soil map of the world. Revised legend. World Soil Resources Report 60, FAO, Rome, 1988. Reprinted with corrections and updates as Technical Paper 20, ISRIC, Wageningen, Netherlands, 1997.

Fischer, K., 1988: Die würmeiszeitliche und stadiale Vergletscherung der Berchtesgadener Alpen (The Weischelian Glaciation of the Berchtesgadener Alps). *Berliner Geographische Abhandlungen*, 47: 207–225.

French, H. M., 1976: *The periglacial environment*. London: Longman.

Frisch, W., Székely, B., Kuhlemann, J., and Dunkl, I., 2000: Geomorphological evolution of the Eastern Alps in response to Miocene tectonics. *Zeitschrift für Geomorphologie N.F.*, 44(1): 103–138.

Haeberli, W., 1978: Sahara dust on the Alps—A short review. *Zeitschrift für Gletscherkunde und Glazialgeologie*, 13(1–2): 206–208.

Hüttl, C., 1997: The influence of different soil types and associations of vegetation on limestone solution in a high-

mountainous region (Zugspitzplatt, Wettersteingebirge, Germany). *Ecologie*, 29(1–2): 83–87.
Hüttl, C., 1999: Steuerungsfaktoren und Quantifizierung der chemischen Verwitterung auf dem Zugspitzplatt (Wettersteingebirge, Deutschland). Controlling factors of chemical weathering and its quantification (karst plateau of Zugspitzplatt, Wetterstein Mts., Germany). *Münchner Geographische Abhandlungen*, 30: 1–171.
ISSS-ISRIC-FAO, 1998: World Reference Base for Soil Resources. FAO, World Soil Resources Report No. 84. Rome.
KIC, 1990: *Munsell Soil Color Charts*. Baltimore: Kollmorgan Instruments Corporation.
Kubiena, W., 1953: *Bestimmungsbuch und Systematik der Böden Europas*. Stuttgart: Enke.
Küfmann, C., 2003a: Erste Ergebnisse zur qualitativen Untersuchung und Quantifizierung rezenter Flugstäube in den Nördlichen Kalkalpen (Wettersteingebirge). First results of studies on eolian dust in the Northern Calcareous Alps (Wettersteingebirge): qualification and quantification. *Mitteilungen der Geographischen Gesellschaft München*, 86: 59–85.
Küfmann, C., 2003b: Soil types and eolian dust in high-mountainous karst of the Northern Calcareous Alps (Zugspitzplatt, Wetterstein Mountains, Germany). *Catena*, 53: 211–227.
Küfmann, C., 2006: Quantifizierung und klimatische Steuerung von rezenten Flugstaubeinträgen auf Schneeoberflächen in den Nördlichen Kalkalpen (Wetterstein-, Karwendelgebirge, Berchtesgadener Alpen, Deutschland). Measurement and climatic control of eolian sedimentation on snow cover surface in the Northern Calcareous Alps (Wetterstein-, Karwendel and Berchtesgadener Alps, Germany). *Zeitschrift für Geomorphologie, N.F.*, 50(2): 245–268.
Kuhlemann, J., Taubald, H., Dunkl, I., and Frisch, W., 1999: Geochemistry of red clays in the Eastern Alps: Remnants of late Miocene soils? *Tübinger Geowissenschaftliche Arbeiten*, A52: 1–166.
Litaor, M. I., 1987: The influence of eolian dust on the genesis of alpine soils in the Front Range, Colorado. *Soil Science Society of American Journal*, 51: 141–146.
Littmann, T., 1991: Recent African dust deposition in West Germany—Sediment characteristics and climatological aspects. *Catena Supplement*, 20: 57–73.
Mahaney, W. C., Sanmugadas, K., North, Y., and Hancock, R. G. V., 1996: Physical and geochemical analysis of a late glacial/Little Ice Age pedostratigraphic complex in the Zillertal Alps, Austria. *Zeitschrift für Geomorphologie N.F.*, 40(4): 447–460.
Mailänder, R., and Veit, H., 2001: Periglacial cover-beds on the Swiss Plateau: indicators of soil, climate, and landscape evolution during the Late Quaternary. *Catena*, 45(4): 251–272.
Matsuoka, N., 1990: The rate of bedrock weathering by frost action: field measurements and a predictive model. *Earth Surface Processes and Landforms*, 15: 73–90.
Mattson, J. O., and Nihlén, T., 1996: The transport of Saharan dust to southern Europe: a scenario. *Journal of Arid Environments*, 32: 111–119.
Mishra, V. K., 1982: Genesis and classification of soils derived from Hauptdolomit (Dolomites) in Kalkalpen and effects of soil type and humus form on some features of forest natural regeneration. Dissertation. Forstwissenschaftliche Fakultät Ludwig-Maximilians Universität München, Germany.
Moore, D. M., and Reynolds, R. C., 1989: *X-ray diffraction and the identification and analysis of clay minerals*. Oxford: Oxford University Press.
Müller, M., 1986: Soils above the timberline in the upper Engadin. *Mitteilungen der deutschen Bodenkundlichen Gesellschaft*, 48: 107–120.
Müller, M., and Peyer, K., 1986: Profile Kloster: raw humus layer on dolomitic Cobbler Talus. *Mitteilungen der deutschen Bodenkundlichen Gesellschaft*, 48: 81–90.
Muhs, D. R., and Benedict, J. B., 2006: Eolian additions to Late Quaternary alpine soils, Indian Peaks Wilderness Area, Colorado Front Range. *Arctic, Antarctic, and Alpine Research*, 38: 120–130.
Munn, L. C., and Spackman, L. K., 1990: Origin of silt-enriched alpine surface mantles in India Basin, Wyoming. *Soil Science Society of America Journal*, 54: 1670–1677.
Pye, K., 1992: Aeolian dust transport and deposition over Crete and adjacent parts of the Mediterranean Sea. *Earth Surface Processes and Landforms*, 17: 271–288.
Reheis, M. C., and Kihl, R., 1995: Dust deposition in southern Nevada and California, 1984–1989: relations to climate, source area and source lithology. *Journal of Geophysical Research*, 100(D5): 8893–8918.
Schlichting, E., Blume, H.-P., and Stahr, K., 1995: *Bodenkundliches Praktikum*. Wien: Blackwell Wissenschaftsverlag.
Schwikowski, M., Seibert, P., Baltensperger, U., and Gäggler, H. W., 1995: A study of an outstanding Saharan dust event at the high-alpine site Jungfraujoch, Switzerland. *Atmospheric Environment*, 29(15): 1829–1842.
Soil Survey Staff, 1994: Keys to soil taxonomy. Sixth edition. Washington, D.C.: U.S. Department of Agriculture, Soil Conservation Service.
Thorn, C. E., and Darmody, R. G., 1980: Contemporary eolian sediments in the alpine zone, Colorado Front Range. *Physical Geography*, 1: 162–171.
Thorn, C. E., and Darmody, R. G., 1985: Grain-size distribution of the insoluble component of contemporary eolian deposits in the alpine zone, Front Range, Colorado, U.S.A. *Arctic and Alpine Research*, 17(4): 433–442.
Trudgill, S. T., 1976: The erosion of limestones under soil and the long term stability of soil-vegetation systems on limestones. *Earth Surface Processes and Landforms*, 1: 31–41.
Veit, H., and Höfner, T., 1993: Permafrost, gelifluction and fluvial sediment transfer in the alpine/subnival ecotone, Central Alps, Austria: present, past and future. *Zeitschrift für Geomorphologie N.F.*, Suppl.-Bd. 92: 71–84.
Wagenbach, D., and Geis, K., 1989: The mineral dust record in a high altitude alpine glacier (Colle Gnifetti, Swiss Alps). *In* Leinen, M., and Sarntheim, M. (eds.), *Paleoclimatology and paleometeorology: modern and past patterns of global atmospheric transport*. New York, Hamburg: Springer Verlag, 543–564.
Wright, J., 2001a: Making loess-sized quartz silt: data from laboratory simulations and implications for sediment transport pathways and the formation of "desert" loess deposits associated with the Sahara. *Quaternary International*, 76/77: 7–19.
Wright, J. S., 2001b: "Desert" loess versus "glacial loess": quartz silt formation, source areas and sediment pathways in the formation of loess deposits. *Geomorphology*, 36: 231–256.
Wright, J., Smith, B. J., and Whalley, W. B., 1998: Mechanism of loess-sized quartz silt production and their relative effectiveness: laboratory simulations. *Geomorphology*, 23: 15–34.

Ms accepted January 2008